# Manganese concentration and low-temperature annealing dependence of $Ga_{1-x}Mn_xAs$ by x-ray absorption spectroscopy

Y. Ishiwata,[1] M. Watanabe,[2] R. Eguchi,[1] T. Takeuchi,[3] Y. Harada,[2] A. Chainani,[1,4] S. Shin,[1,2] T. Hayashi,[1] Y. Hashimoto,[1] S. Katsumoto,[1,5] and Y. Iye[1,5]

[1]*Institute for Solid State Physics, University of Tokyo, Kashiwanoha, Kashiwa, Chiba 277-8581, Japan*

[2]*RIKEN/SPring-8, Kouto, Mikazuki-cho, Sayo-gun, Hyogo 679-5143, Japan*

[3]*Department of Applied Physics, Tokyo University of Science, Kagurazaka, Shinjyuku-ku, Tokyo 162-8601, Japan*

[4]*Institute for Plasma Research, Bhat, Gandhinagar-382 428, India*

[5]*CREST, Japan Science and Technology Corporation, Mejiro, Tokyo 171-0031, Japan*

(Received 15 October 2001; revised manuscript received 20 February 2002; published 22 May 2002)

The Mn-site-projected electronic structure of the diluted magnetic semiconductors $Ga_{1-x}Mn_xAs$ ($x=0.032$, 0.038, 0.047, 0.052, 0.058) of as-grown and low-temperature (LT) annealed samples are systematically studied using high-resolution Mn $2p$ absorption spectroscopy. The study exhibits coexistence of the ferromagnetic $Mn^{2+}$ ion and the paramagnetic Mn-As complex that transforms into the ferromagnetic component with LT annealing. The ratio of ferromagnetic to paramagnetic components is directly related to the $x$ dependence of the hole density and ferromagnetic critical temperature.

DOI: 10.1103/PhysRevB.65.233201 PACS number(s): 75.50.Pp, 71.28.+d, 78.70.Dm, 79.60.−i

Carrier-induced ferromagnetism in III-V based diluted magnetic semiconductors,[1] which has been utilized for the recent successful control of ferromagnetism by external parameter such as light illumination[2] or electric field,[3] is now attracting much attention although the detailed mechanism is still under debate.[1,4–12] Especially $Ga_{1-x}Mn_xAs$ has comparatively high ferromagnetic critical temperature ($T_c$) and excellent connectivity to the elaborated GaAs-based superstructures. Several experiments on local electronic structure around Mn ions in $Ga_{1-x}Mn_xAs$ have already been reported,[13–16] but they have been performed for the samples with Mn content $x$ below the value corresponding to the maximum of $T_c$. Hence a systematic direct measurement of the local electronic structure across the $T_c$ maximum is desired to clarify the mechanism of the carrier-induced ferromagnetism. Here ''direct'' means a signal labeled unambiguously as one of Mn atoms.

The $2p$ x-ray absorption spectroscopy (XAS) of $3d$ transition-metal compounds is a powerful technique for the direct probing of the $3d$ valence electronic structure due to the dipole selection rule.[17,18] The transitions are made into the screening states, so that the spectrum is unaffected by the core-hole potential in contrast to core-level photoemission. Especially in diluted systems, XAS has great advantages for little surface effect. Recently it was found that low-temperature (LT) annealing after the growth of $Ga_{1-x}Mn_xAs$ crystals greatly increases $T_c$ and the hole density ($n_p$) without influencing $x$.[19,20] This is mostly due to the removal of excess As atoms that operate as deep donors.[21,22] This technique should also be useful for the systematic study.

In this paper we report systematic measurements of the site-projected Mn $3d$ states of $Ga_{1-x}Mn_xAs$ by high-resolution Mn $2p \rightarrow 3d$ XAS across the $T_c$ maximum on as-grown and LT-annealed samples. Our study exhibits that the XAS spectrum consists of two components: (i) one from the ferromagnetic $Mn^{2+}$ ions and (ii) the other from the metastable paramagnetic Mn ions coupled to excess As atoms. We found that the latter component is transformed into the former by the LT annealing. The ratio of ferromagnetic to paramagnetic components is directly related to the $x$ dependence of the $n_p$ and $T_c$.

$Ga_{1-x}Mn_xAs$ films were grown by molecular-beam epitaxy on semiinsulating (001) GaAs substrates around 230 °C under As-rich conditions. The growth parameters were optimized so as to obtain the highest $T_c$ for each $x$. To estimate the nominal $x$'s in as-grown samples, the lattice constants were measured from the x-ray diffraction (XRD) of the index (004). The LT annealing ($T=260$ °C) was carried out in the environment of nitrogen gas. The annealing time was fixed to 15 min. There was no increase in full width at half maximum of the (004) XRD peak, which indicates that the annealing caused no significant inhomogeneity in the films. The electrical transport was measured by a conventional ac bridge with van der Pauw method. The $n_p$ was estimated from the Hall coefficient at room temperature (RT) and the $T_c$ was determined from magnetization measurement. Details of the samples used in the present study are given in Table I. XAS was measured in total photon yield mode. The samples were 200 nm thick, which is enough to absorb all incident photons. XAS was performed using a soft-x-ray spectrometer installed at the undulator beamline BL-2C in the photon fac

TABLE I. The $n_p$ ($cm^{-3}$) and $T_c$ (K) for the as-grown and LT-annealed samples of $Ga_{1-x}Mn_xAs$ ($x=0.032$, 0.038, 0.047, 0.052, 0.058).

| | As-grown sample | | LT-annealed sample | |
|---|---|---|---|---|
| $x$ | $n_p$ ($cm^{-3}$) | $T_c$ (K) | $n_p$ ($cm^{-3}$) | $T_c$ (K) |
| 0.032 | $1.2\times10^{19}$ | | $1.6\times10^{19}$ | 30 |
| 0.038 | $3.4\times10^{19}$ | 30 | $7.5\times10^{19}$ | 60 |
| 0.047 | $5.9\times10^{19}$ | 55 | $1.5\times10^{20}$ | 100 |
| 0.052 | $2.1\times10^{19}$ | 30 | $6.2\times10^{19}$ | 85 |
| 0.058 | $6.1\times10^{19}$ | 45 | $1.1\times10^{20}$ | 80 |

 

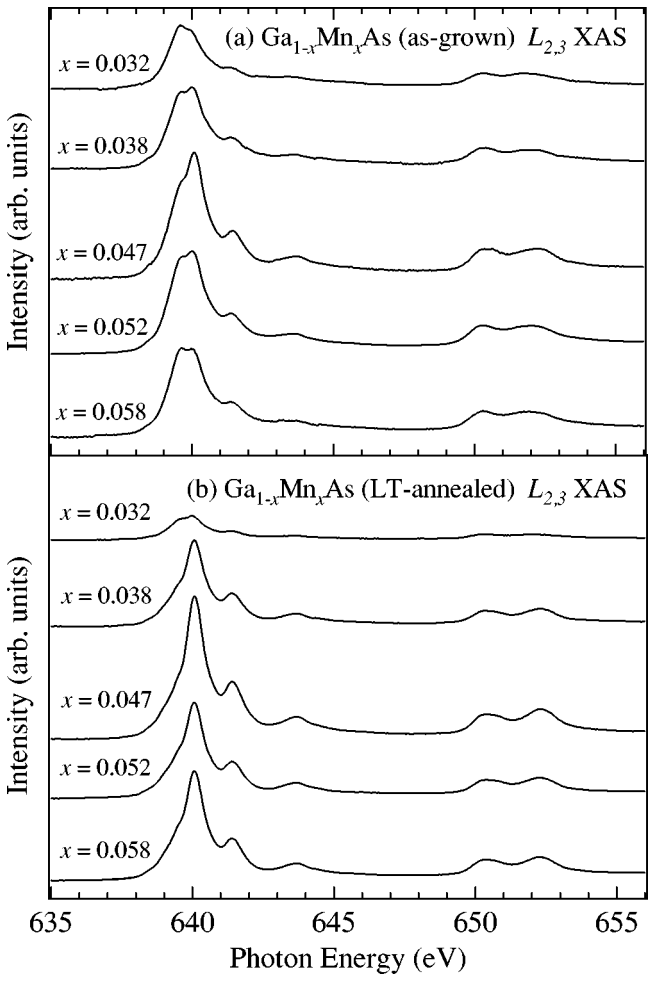


FIG. 1. Mn $2p$ XAS spectra for (a) as-grown and (b) LT-annealed $Ga_{1-x}Mn_xAs$ ($x=0.032$, 0.038, 0.047, 0.052, 0.058) at RT.

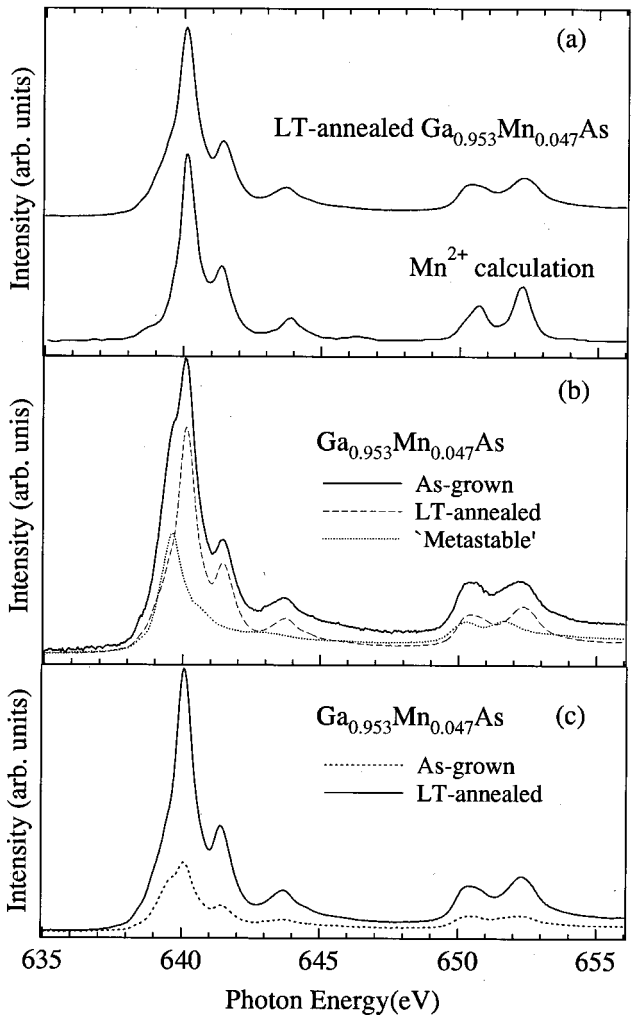


FIG. 2. (a) Comparison between Mn $2p$ XAS spectra for LT-annealed $Ga_{0.953}Mn_{0.047}As$ sample and the calculation based on atomic multiplet theory for $Mn^{2+}$ ($d^5$) in tetrahedral coordination for 10 $Dq=0.5$ eV.[17] (b) An example of Mn $2p$ XAS spectra for $Ga_{1-x}Mn_xAs$ resolved into two components. Solid line is Mn $2p$ XAS spectrum for as-grown $Ga_{0.953}Mn_{0.047}As$ sample. Dashed line is the scaled spectrum for the LT-annealed sample and dotted line is the ''metastable'' component. (c) LT annealing dependence of the XAS intensity for $x=0.047$ sample. The annealed spectrum (solid line) increases relative to the as-grown one (dotted line).

tory of KEK. Synchrotron radiation was monochromatized using a varied-line-spacing plane grating, whose energy resolution was better than 0.1 eV at 650 eV. All measurements were performed at RT.

Figures 1(a) and 1(b) show XAS spectra across Mn $2p$ threshold of as-grown and LT-annealed $Ga_{1-x}Mn_xAs$ ($x=0.032$, 0.038, 0.047, 0.052, 0.058), respectively. The spectra are normalized for incident photon flux. The features around 640 eV and 651 eV correspond to the $L_3$ ($2p_{3/2}\rightarrow 3d$) and $L_2$ ($2p_{1/2}\rightarrow 3d$) levels. The as-grown samples show a main peak doublet structure for the $L_3$ levels at 639.5 eV and 640 eV. In contrast, the LT-annealed samples show a single main peak at 640 eV, except for the $x=0.032$. The LT-annealed sample for $x=0.047$ exhibits a spectral shape very similar to the calculation based on atomic multiplet theory for $Mn^{2+}$ ($d^5$) in tetrahedral coordination for the case with crystal-field strength ($10\ Dq$)$=0.5$ eV [see Fig. 2(a)].[17] This means that the hole is mainly created in As $4p$ orbital for $Ga_{1-x}Mn_xAs$.

The reduction in intensity of the feature at 639.5 eV with LT annealing is indicative of the presence of two types of Mn ions in the as-grown samples. Using the LT-annealed spectrum for $x=0.047$ (''intrinsic;'' dashed line), the difference spectrum (''metastable;'' dotted line) is obtained by the subtraction as shown in Fig. 2(b). Transformation from ''metastable'' to ''intrinsic'' on LT annealing shows the alternation in the local environment around Mn. Since LT annealing probably acts on evaporation of the excess As atoms,[19,20] the ''metastable'' Mn ions are suggested to be forming Mn-As complexes. The ''metastable'' component resembles the broadened spectrum for the $d^5$ configuration shifted to 0.5 eV lower energy rather than the $d^4$ configuration.[17,18] The difference between the intrinsic and metastable components is probably due to two effects of Mn-As complex: self-compensation of hole and local lattice polarization between Mn acceptor and excess As donor.

Since the LT annealing results in no loss of Mn

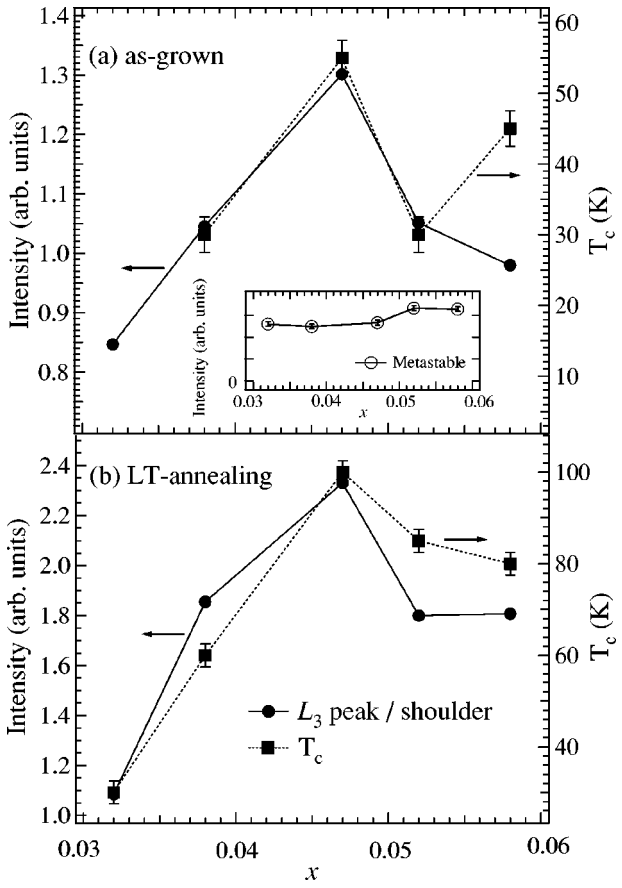


FIG. 3. $x$ dependence of the intensity ratio of the peak at 640 eV to the feature (shoulder) at 639.5 eV as well as $T_c$ for (a) as-grown and (b) LT-annealed $Ga_{1-x}Mn_xAs$ ($x=0.032$, 0.038, 0.047, 0.052, 0.058). Inset shows $x$ dependence of the integrated intensity of ''metastable'' for the as-grown samples.

content,[19,20] we expected the total intensity in the spectra for the same composition to be conserved before and after annealing. Figure 2(c), however, shows enhancement in intensity upon LT annealing compared to the as-grown spectrum for $x=0.047$. The same behavior was observed for all compositions. There are two possibilities for the large difference. One is the absorption of the excess As in the Mn $2p$ region. The other is the lower valence of the metastable Mn site as judged from the chemical shift to lower energy. When occupation of $d$ orbital is larger, the metal $2p$ absorption is generally reduced.

The $x$ dependence of intrinsic and metastable Mn sites should be discussed in order to explore the relation to that of $n_p$ or $T_c$. For the quantitative discussion, one can consider the intensity ratio of the peak at 640 eV to the feature (shoulder) at 639.5 eV. Figures 3(a) and 3(b) illustrate $x$ dependence of the intensity ratio before and after annealing, plotted along with the $T_c$'s of the samples for comparison. Inset shows the integrated intensity of metastable component before annealing. It is found that the $x$ dependence of the intensity ratio fairly follows the $T_c$ for both as-grown and LT-annealed materials. Figures 3(a) and 3(b) clearly show that the intensity ratio has strong correlation with $T_c$. However, the intensity of metastable component is almost constant for varying $x$. As reported by the magnetization measurements, the metallic samples with $x$ close to the $T_c$ maximum have shown a dominant ferromagnetic contribution, whereas the insulating samples have exhibited that the paramagnetic contribution reached almost 50% of total saturation magnetization.[1,6,23,24] Hence we can conclude that ''intrinsic'' component corresponds to the ferromagnetic component, while the ''metastable'' one conforms to the paramagnetic component.

This is the first observation of a microscopic distinction between the ferromagnetic and paramagnetic Mn ions. This does not contradict with the results of electron paramagnetic resonance (EPR) that there is no neutral Mn states in $Ga_{1-x}Mn_xAs$ with $x$ less than 0.01.[13] The paramagnetic Mn ions also have $d^5$-like configuration and the shift in the EPR spectra from those of ferromagnetic ones should be small and buried in the broad signal. It should be also noticed that the Mn $2p$ x-ray magnetic circular dichroism study of a ferromagnetic sample showed a structure similar to the LT-annealed spectrum in Fig. 2.[16] On the other hand, $Ga_{1-x}Mn_xAs$ undergoes an insulator-to-metal-to-insulator transition (IMIT) with increasing $x$ from the dilute limit.[5,6,20,23,24] Figure 3 also reveals that the ratio of $Mn^{2+}$ ions to metastable Mn-As complexes becomes maximum for the metallic sample with $x=0.047$ showing the highest $n_p$ (see Table I). Hence it is almost apparent that the IMIT directly comes from this ratio related to excess As.

Since the ferromagnetic component is clarified to be high-spin $Mn^{2+}$ ion, the ferromagnetism is mediated by As $4p$ hole rather than Mn $d$ hole. Whether As $4p$ hole is mainly activated or not is unclear. This is because the XAS reflects local electronic structure around $Mn^{2+}$ ion. It should be noted that As $4p$ hole is expected to have a relatively large radius even if As $4p$ hole is bound to $Mn^{2+}$ ion.

In conclusion, we have systematically studied the local electronic structure around Mn in $Ga_{1-x}Mn_xAs$ by high-resolution Mn $2p$ XAS. From a comparison of as-grown and LT-annealed samples, the ''ferromagnetic'' electronic configuration is assigned to high-spin $Mn^{2+}$ ion. In addition, we identify metastable paramagnetic component due to coupling with excess As, which transforms into the ferromagnetic component with LT annealing. The ratio of ferromagnetic $Mn^{2+}$ ions to paramagnetic Mn-As complexes is scaled with the $x$ dependence of the $n_p$ and $T_c$.

We would like to thank A. Kotani, K. Kobayashi, K. Kanai, T. Ishikawa for helpful discussions and A. Yagishita for technical support. This work was partly supported by a Grant-in-Aid for the Scientific Research from the Ministry of Education, Science, Sports and Culture, Japan.

[1] H. Ohno, Science **281**, 951 (1998).
[2] S. Koshihara, A. Oiwa, M. Hirasawa, S. Katsumoto, Y. Iye, C. Urano, H. Takagi, and H. Munekata, Phys. Rev. Lett. **78**, 4617 (1997).
[3] H. Ohno, D. Chiba, F. Matsukura, T. Omiya, E. Abe, T. Dietl, Y. Ohno, and K. Ohtani, Nature (London) **408**, 944 (2000).
[4] H. Ohno, H. Munekata, T. Penney, S. von Molnár, and L. L. Chang, Phys. Rev. Lett. **68**, 2664 (1992).
[5] A. Van Esch, L. Van Bockstal, J. De Boeck, G. Verbanck, A. S. van Steenbergen, P. J. Wellmann, B. Grietens, R. Bogaerts, F. Herlach, and G. Borghs, Phys. Rev. B **56**, 13 103 (1997).
[6] F. Matsukura, H. Ohno, A. Shen, and Y. Sugawara, Phys. Rev. B **57**, R2037 (1998).
[7] H. Akai, Phys. Rev. Lett. **81**, 3002 (1998).
[8] B. Beschoten, P. A. Crowell, I. Malajovich, D. D. Awschalom, F. Matsukura, A. Shen, and H. Ohno, Phys. Rev. Lett. **83**, 3073 (1999).
[9] T. Dietl, H. Ohno, F. Matsukura, J. Cibert, and D. Ferrand, Science **287**, 1019 (2000).
[10] J. König, H.-H. Lin, and A. H. MacDonald, Phys. Rev. Lett. **84**, 5628 (2000).
[11] J. Inoue, S. Nonoyama, and H. Itoh, Phys. Rev. Lett. **85**, 4610 (2000).
[12] T. Dietl, H. Ohno, and F. Matsukura, Phys. Rev. B **63**, 195205 (2001).
[13] J. Szczytko, A. Twardowski, K. Świątek, M. Palczewska, M. Tanaka, T. Hayashi, and K. Ando, Phys. Rev. B **60**, 8304 (1999).
[14] J. Okabayashi, A. Kimura, O. Rader, T. Mizokawa, A. Fujimori, T. Hayashi, and M. Tanaka, Phys. Rev. B **58**, R4211 (1998).
[15] J. Okabayashi, A. Kimura, T. Mizokawa, A. Fujimori, T. Hayashi, and M. Tanaka, Phys. Rev. B **59**, R2486 (1999).
[16] H. Ohldag, V. Solinus, F. U. Hillebrecht, J. B. Goedkoop, M. Finazzi, F. Matsukura, and H. Ohno, Appl. Phys. Lett. **76**, 2928 (2000).
[17] G. van der Laan and I. W. Kirkman, J. Phys.: Condens. Matter **4**, 4189 (1992).
[18] F. M. F. de Groot, J. C. Fuggle, B. T. Thole, and G. A. Sawatzky, Phys. Rev. B **42**, 5459 (1990).
[19] T. Hayashi, Y. Hashimoto, S. Katsumoto, and Y. Iye, Appl. Phys. Lett. **78**, 1691 (2001).
[20] S. Katsumoto, T. Hayashi, Y. Hashimoto, Y. Iye, Y. Ishiwata, M. Watanabe, R. Eguchi, T. Takeuchi, Y. Harada, S. Shin, and K. Hirakawa, Mater. Sci. Eng., B **84**, 88 (2001).
[21] S. O'Hagan and M. Missous, J. Appl. Phys. **75**, 7835 (1994).
[22] H. Shimizu, T. Hayashi, T. Nishinaga, and M. Tanaka, Appl. Phys. Lett. **74**, 398 (1999).
[23] A. Oiwa, S. Katsumoto, A. Endo, M. Hirasawa, Y. Iye, H. Ohno, F. Matsukura, A. Shen, and Y. Sugawara, Solid State Commun. **103**, 209 (1997).
[24] Y. Iye, A. Oiwa, A. Endo, S. Katsumoto, F. Matsukura, A. Shen, H. Ohno, and H. Munekata, Mater. Sci. Eng., B **63**, 88 (1999).